


Research Article

A Full-Duplex Decode-and-Forward Relaying Approach Based on QAM Constellation Suitable for Small-Size Devices

Xinhai Song ¹, Haiyang Ding,² Liang He,¹ and Zhuang Miao¹

¹College of Engineering, Xi'an International University, Xi'an, Shaanxi 710077, China

²School of Information and Communications, National University of Defense Technology, Wuhan, Hubei 430010, China

Correspondence should be addressed to Xinhai Song; drunkentinker@foxmail.com

Received 30 September 2022; Revised 13 February 2023; Accepted 1 March 2023; Published 17 April 2023

Academic Editor: Quanzhong Li

Copyright © 2023 Xinhai Song et al. This is an open access article distributed under the Creative Commons Attribution License, which permits unrestricted use, distribution, and reproduction in any medium, provided the original work is properly cited.

The explosive growth of the Internet of Things (IoT) is putting higher requirements for the performance of co-time co-frequency full-duplex relaying (CCFD-R) due to small-size devices appearing in abundance. In this paper, we present a novel CCFD-R approach with very low complexity to deal with the issue above. Based on the orthogonality of its two components, a distributed usage mode of quadrature amplitude modulation (QAM) constellation is proposed to perform self-interference cancellation (SIC) without the complicated processing modules, as used widely in traditional full-duplex techniques. Instead of the conventional practice of assigning the entire QAM constellation to only one communication node, our scheme (termed as QAM-R) splits the constellation into two parts and further assigns them to different communication nodes, respectively. With the principle above, the mapping pattern and the frame format are carefully designed. Then, the corresponding signal model is established and the approximation of end-to-end bit error probability (BEP) is derived. Finally, numerical simulations validate the theoretical analysis and show that QAM-R can balance spectrum effectiveness and transmission reliability very well and, especially, performs even better in the low range of signal noise ratio (SNR) when adopting higher-order QAM constellations.

1. Introduction

Owing to the absence of spectrum resources with the tremendous growth of mobile traffic, co-time co-frequency full-duplex (CCFD) has attracted significant attentions from both academic and industrial societies. Accordingly, CCFD relaying (CCFD-R) becomes a promising technique for integrating the merits of both relaying and CCFD. However, while CCFD-R significantly improves the spectral efficiency of relay systems, it also leads to more complicated self-interference (SI) problems than normal CCFD communications, rendering SI cancellation (SIC) the vital enabling techniques in this field [1].

The existing SIC techniques can be generally divided into two categories, i.e., passive suppression and active cancellation [2]. The former mainly operates in the propagation-domain to electromagnetically isolate the antennas between the transmitter and the receiver [3] and, on the contrast, the latter takes effect in analog-domain and/or digital-domain

by means of various sophisticated signal processing techniques [4, 5]. Although these SIC techniques have good performance, they are mainly designed for traditional cellular networks on account of the path dependence. Nowadays, the Internet of Things (IoT) is playing an increasingly important role in mobile communications with the arrival of 5G and its evolution to 6G [6]. Due to the constraints of low power, cost, complexity, and so on, the IoT devices inevitably put forward higher requirements for IoT networks when implementing CCFD-R communication. Especially, as an important type of IoT devices, the massive small-size devices (e.g., a sea of sensors) even bring new research challenges for CCFD-R in IoT networks because of the strict limitations of both space and energy. For instance, it has been one of the critical issues for various sensors how to work in CCFD-R mode, particularly, for the rising simultaneous wireless information and power transfer (SWIPT) IoT systems [7–9]. From the above, the aforementioned SIC techniques are surely ill-suited to be directly incorporated into IoT relaying

and should be improved to match the particularities of the small-size devices. Apparently, due to lack of enough space for antenna isolation, it is indeed a little difficult for small-size devices to apply the SIC techniques in the propagation-domain. Similarly, the SIC techniques in analog-domain are neither an appealing approach because the additional analog circuits need not only high power consumption but also enough space requirements. Hence, looking for novel digital-domain SIC techniques might be quite a promising technical direction for small-size devices.

Aiming at a low-complexity solution to CCFD-R suitable for the IoT networks with small-size devices, we try to design a new approach based on distributed quadrature amplitude modulation (QAM) constellation in this paper. This thought originally came from the quadrature signals-based cooperative diversity (QSCD) to distinguish different users in cooperative systems by utilizing the property that the inner product of the two components of QAM constellation is zero [10, 11]. QSCD-type techniques are very appropriate for small-size devices by virtue of the easy implement and low cost, but they still work in half-duplex (HD) mode. Fortunately, a similar technique using an optical in-phase/quadrature (IQ) modulator was recently introduced in CCFD wireless communications [12]. Although it is not dedicated to designing for relay systems, the practice of separately processing IQ modulation is very instructive. Inspired by this, we propose a very low-complexity QAM-based CCFD-R (abbreviated as QAM-R) system through improving the above QSCD-type techniques. The main idea is to split the QAM constellation into two parts and further assign them to the source and relay nodes, respectively, to realize CCFD-R. The major contributions of this paper are as follows:

- (1) The proposal of the distributed usage mode of QAM constellation to guarantee the orthogonality of the transmitted and received signals at the relay node.
- (2) The design of the corresponding relaying scheme for the typical three-node relay system, mainly including the mapping constellation and the frame format.
- (3) The establishment of the corresponding signals model and the approximation of end-to-end bit error probability (BEP) of the proposed system.

Apparently, QAM-R is essentially just the innovative use of QAM constellation, without the need for complicated SIC modules such as in traditional CCFD-R systems, so it is immune to the size of transceivers and, meanwhile, has the advantage of low cost. Both the theoretical analysis and the digital simulations in this paper show that QAM-R can also provide a good compromise between spectrum effectiveness and transmission reliability. Hence, the proposed approach is very suitable for the massive small-size devices emerging with the IoT era arrival.

The rest of this paper is organized as follows. To begin with, the relaying scheme for the typical three-node relay system is carefully designed in Section 2. Then, the corresponding signal model is established and the approximation of end-to-end BEP is derived in Section 3. Next, numerical

simulations are carried out to verify the theoretical analysis in Section 4. Finally, we draw the main conclusions of the whole paper in Section 5.

2. System Model and Relaying Scheme

Consider the typical relay system model shown in Figure 1, in which one source node (SN) transmits information to one destination node (DN) via one relay node (RN), and all the three nodes are set as small-size devices equipped with one antenna, respectively. Depending on the processing at the relay node, the relay protocol can be broadly classified as amplify-and-forward (AF) and decode-and-forward (DF), and in this paper, we choose the latter.

It should be pointed out here that RN can also be equipped with two antennas (one for transmitting and the other for receiving), which have the same effect as a single antenna with a circulator to implement full-duplex operation in theory. We assume reasonably there is no direct-link between SN and DN due to serious obstacles usually existing in the environments in which the IoT devices (such as SigFox and LoRa) are generally far apart from each other and, at the same time, work at a very low power pattern. In addition, we assume the symbols $h_{S,R}$ and $h_{R,D}$ capture the channel fading coefficients (CFCs) between the corresponding two adjacent nodes as depicted in Figure 1.

Referring to the aforesaid QSCD-type techniques which assign the in-phase and quadrature components of QAM signals to different users at a certain cooperative node, respectively, our design principle is to split the entire QAM constellation into two parts, i.e., one for SN and the other for RN. For instance, the in-phase component is assigned to SN to carry information, and the quadrature component is assigned to RN, and vice versa. This means that the modulation of QAM-R is M-ary QAM (MQAM) for the whole system but M-ary pulse amplitude modulation (MPAM) for SN and RN (note that the modulation order of the former is equal to the square of the latter for our study). Further, unlike QSCD-type techniques which transmit the resultant information of cooperative users through the respective multiple access channels, we let SN and RN operate simultaneously on the same frequency band and, especially, let RN listen and transmit in CCFD mode. Unfortunately, this practice will inevitably cause the QAM constellation losing orthogonality at RN and further bring SI to the whole system, as is not occurred for QSCD-type techniques since they worked in HD mode. But, according to our studies, this critical problem can be solved through reversely rotating the transmitted signals of SN by the phase of $h_{S,R}$ when they are emitted. Thus, the influence of $h_{S,R}$ is hedged, and the orthogonality of QAM constellation at RN is then guaranteed. That is, the inner product of the transmitted signal and the received signal at RN is zero, and then, theoretically, the QAM-R solution is formed without SI at RN.

Based on the above, the detailed relaying scheme of QAM-R, mainly including the mapping constellation and the frame format, is designed as shown in Figure 2 (taking 4PAM/16-QAM modulation as an example), where \tilde{x}_S and \tilde{x}_R are the constellation points of SN and RN and,

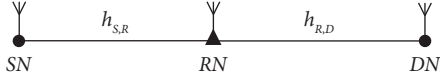


FIGURE 1: System model.

accordingly, $2d_s$ and $2d_r$ are the minimum Euclidean distance between the respective different constellation points of SN and RN. First, Figure 2(a) illustrates the mapping constellations for SN and RN. Specifically, the left subpicture (1) depicts that the SN's data bits b_s are fed to the in-phase component, and the right subpicture (2) depicts that the SN's regenerated data bits at RN (i.e., \tilde{b}_s^R) are fed to the quadrature component. According to the design idea, the modulated signal of SN (i.e., \tilde{x}_s) should be offset by $-\theta_{s,r}$ before being transmitted, for maintaining the orthogonality of the QAM constellation at RN. Thus, SN and RN would simultaneously transmit data on the same frequency band without SI in theory, and particularly, RN can work in CCFD mode. Second, Figure 2(b) illustrates the frame structure corresponding to Figure 2(a). In the first symbol interval, SN just transmits its own information on the in-phase component. In the successive symbol intervals, SN still transmits its information in the same way, and meanwhile, RN decodes the received signal at the immediately previous symbol interval of SN and forwards it to DN on the quadrature component. In the last symbol interval, only RN decodes and forwards the last immediately previous received signal of SN to DN on the quadrature component.

In general, the relay system works in CCFD mode, except for the first and last symbol interval which can be ignored since they are very small fraction of the whole frame.

3. Signal Model and End-to-End BEP Analysis

We first establish the mathematical model of transmitted and received signals for QAM-R. Clearly, the entire communication process consists of two phases: phase I in which SN sends the data to RN and phase II in which RN detects and forwards the data of SN to DN. Assume quasi-static flat Rayleigh channel fading, and then the index t of the CFC items $h_{s,r}(t)$ and $h_{r,d}(t)$ can be omitted since they remain unchanged throughout the whole frame.

During phase I, let $x_s(t)$ be the baseband equivalent transmitted signal of SN for a certain symbol interval within a frame, and then the baseband received signal at RN is

$$y_r(t) = h_{s,r}x_s(t) + w_r(t), \quad (1)$$

where the CFC item $h_{s,r} \sim CN(0, \sigma_{s,r}^2)$ and the additive white Gaussian noise (AWGN) item $w_r(t) \sim CN(0, N_0)$.

Assume $\tilde{x}_s(t)$ is information symbol modulated by SN's data $b_s(t)$ as shown in the left subpicture (2) of Figure 2(a) and SN knows the CFC (i.e., $h_{s,r}$) between SN and RN, $x_s(t)$ can be finally expressed as $\tilde{x}_s(t)$ rotated by the opposite of the angle of $h_{s,r}$ (i.e., $-\theta_{s,r}$), that is

$$x_s(t) = (h_{s,r}^* / |h_{s,r}(t)|) \tilde{x}_s(t), \quad (2)$$

where the superscript $*$ stands for conjugate of a complex number and $|\bullet|$ the modulus of a complex number.

Using maximum likelihood (ML) detection at RN on the in-phase component, the corresponding reproduced data of SN can be written as

$$\hat{x}_s^R(t) = \underset{x_s^R(t) \in \mathcal{M}}{\operatorname{argmin}} \left\| \tilde{y}_r(t), x_s^R(t) \right\|^2, \quad (3)$$

where $\|\bullet\|$ denotes the Euclidean distance of two points, \mathcal{M} denotes the set of modulation constellation points and decision statistics $y_r(t)$ is

$$\tilde{y}_r(t) = \frac{\Re\{y_r(t)\}}{|h_{s,r}|}, \quad (4)$$

where $\Re(\bullet)$ denotes the real part of a complex number.

Next, the communication process moves to phase II, in which $\hat{x}_s^R(t)$ is decoded as $\tilde{b}_s^R(t)$ and then fed to the quadrature component of QAM constellation as shown in the right subpicture of Figure 2(a). In fact, the above practice is equivalent to multiplying $\hat{x}_s^R(t)$ by imaginary number j , thus the baseband transmitted symbol of RN at the immediately next symbol interval can be expressed as

$$\begin{aligned} x_r(t+T) &= \tilde{x}_r(t+T) \\ &= j\tilde{b}_s^R(t), \end{aligned} \quad (5)$$

where T means the symbol duration. According, the baseband received signal at DN is

$$y_d(t+T) = h_{r,d}x_r(t+T) + w_d(t+T), \quad (6)$$

where the CFC item $h_{r,d} \sim CN(0, \sigma_{r,d}^2)$ and the AWGN item $w_d(t+T) \sim CN(0, N_0)$.

Go on with ML detection at DN on the quadrature component, the reproduced data from RN is then, with DN knowing the CFC (i.e., $h_{r,d}$) between RN and DN, given as

$$\hat{x}_s^D(t+T) = \underset{x_s^D(t+T) \in \mathcal{M}}{\operatorname{argmin}} \left\| \tilde{y}_d(t+T), x_s^D(t+T) \right\|^2, \quad (7)$$

where the decision statistics $\tilde{y}_d(t+T)$ is

$$\tilde{y}_d(t+T) = \frac{\Im\{h_{r,d}^* y_d(t+T)\}}{|h_{r,d}|^2}, \quad (8)$$

where $\Im(\bullet)$ denotes the image part of a complex number and then $\tilde{b}_s^D(t+T)$ (i.e., the final estimate of $b_s(t)$ at DN) can be obtained through decoding $\hat{x}_s^D(t+T)$ in the end.

Now, choosing an arbitrary entire communication process, we analyze the end-to-end BEP performance. For brevity, the index t and the symbol duration T are omitted below.

First thing first, we analyze the end-to-end symbol error probability (SEP). Let A_{ik} denote the event that the constellation point i is detected as the point k for SN during phase I, and similarly, B_{ki} denote the event that the constellation point k is detected as the point i for RN during phase II. Then, the instantaneous end-to-end SEP can be written as

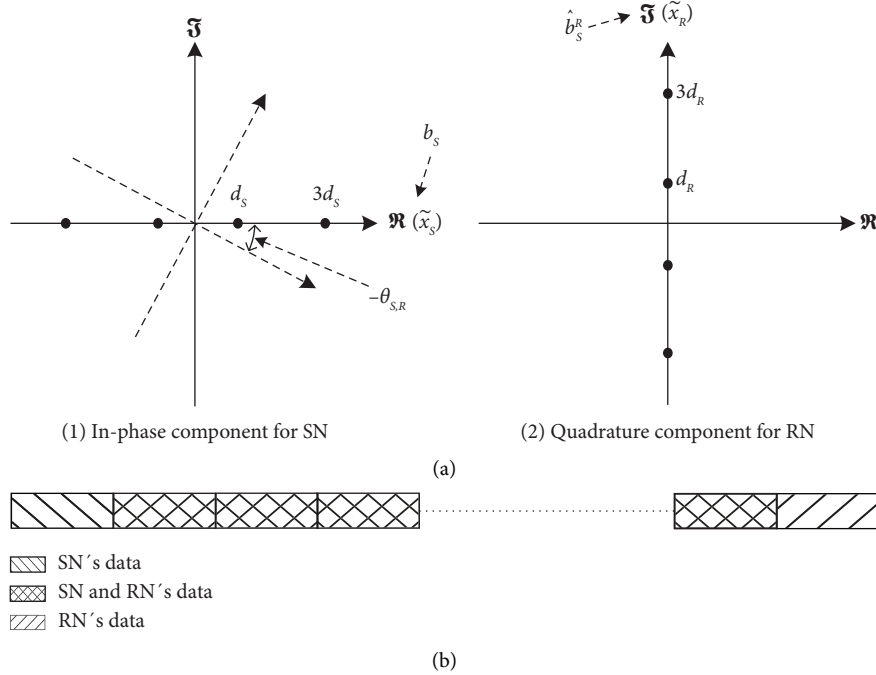


FIGURE 2: Mapping constellation and frame format. (a) Mapping constellation. (b) Frame format.

$$\begin{aligned}
 P_e^c &= 1 - \Pr \left\{ \frac{1}{M} \bigcup_{i=1}^M \bigcup_{k=1}^M (A_{ik} \cap B_{ki}) \right\} \\
 &= 1 - \Pr \left\{ \frac{1}{M} \sum_{i=1}^M \sum_{k=1}^M (A_{ik} \cap B_{ki}) \right\}, \tag{9}
 \end{aligned}$$

where $\Pr(\bullet)$ means the probability of an event and M is the modulation order of arbitrary component of the QAM constellation (note that the design principle of QAM-R implies that the modulation orders of the two components of QAM constellation are the same).

Although (9) provides an exact solution to end-to-end SEP of QAM-R, it is difficult to obtain the result in exact form. However, considering that it is the most likely case for

the adjacent decision region to make an error, we approximate the above p_e^c as

$$\begin{aligned}
 P_e^c &\approx 1 - \frac{1}{M} \Pr \left\{ \sum_{i=1}^1 \sum_{k=i}^{i+1} (A_{ik} \cap B_{ki}) \right. \\
 &\quad \left. + \sum_{i=2}^{M-1} \sum_{k=i-1}^{i+1} (A_{ik} \cap B_{ki}) + \sum_{i=M}^M \sum_{k=i-1}^i (A_{ik} \cap B_{ki}) \right\}. \tag{10}
 \end{aligned}$$

Based on the detection rule in (3) and (7) as well as the fact that $h_{s,R}$ and $h_{r,D}$ are independent of each other, the instantaneous end-to-end SEP in (10) can be calculated, with the basic result ([13], equations (6, 19)), as follows:

$$\begin{aligned}
 P_e^c &\approx 1 - \frac{1}{M} \left\{ 2 \left[\mathcal{Q} \left(\sqrt{|h_{s,R}|^2 d_s^2 / N_0} \right) \mathcal{Q} \left(\sqrt{|h_{r,D}|^2 d_r^2 / N_0} \right) \right. \right. \\
 &\quad \left. \left. + \left(1 - \mathcal{Q} \left(\sqrt{|h_{s,R}|^2 d_s^2 / N_0} \right) \right) \left(1 - \mathcal{Q} \left(\sqrt{|h_{r,D}|^2 d_r^2 / N_0} \right) \right) \right] \right. \\
 &\quad \left. + (M-2) \left[2 \mathcal{Q} \left(\sqrt{|h_{s,R}|^2 d_s^2 / N_0} \right) \mathcal{Q} \left(\sqrt{|h_{r,D}|^2 d_r^2 / N_0} \right) \right. \right. \\
 &\quad \left. \left. + \left(1 - 2 \mathcal{Q} \left(\sqrt{|h_{s,R}|^2 d_s^2 / N_0} \right) \right) \left(1 - 2 \mathcal{Q} \left(\sqrt{|h_{r,D}|^2 d_r^2 / N_0} \right) \right) \right] \right\}. \tag{11}
 \end{aligned}$$

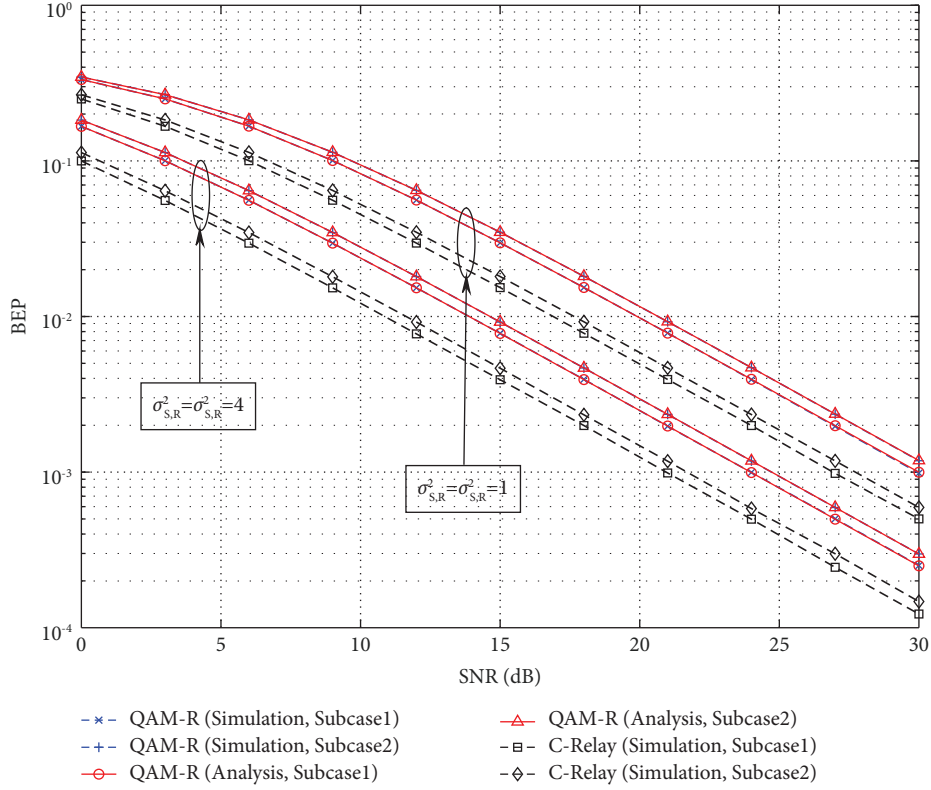


FIGURE 3: Performance comparison between QAM-R and C-Relay under Case 1.

According to the relation between the minimum signal distance and the average energy per symbol ([14], equation (2)), the d_S and d_R in Figure 2(a) can be written as

$$\begin{cases} d_S = \sqrt{\frac{3E_S}{M^2 - 1}}, \\ d_R = \sqrt{\frac{3E_R}{M^2 - 1}}, \end{cases} \quad (12)$$

where E_S and E_R denotes the average energy per symbol of SN and RN, respectively.

Let the received instantaneous signal noise ratios (SNRs) associated with phase I and phase II are $\gamma_{S,R} = (E_S/N_0)|h_{S,R}|^2$ and $\gamma_{R,D} = (E_R/N_0)|h_{R,D}|^2$, thus the responding average SNRs are $\bar{\gamma}_{S,R} = (E_S/N_0)\sigma_{S,R}^2$ and $\bar{\gamma}_{R,D} = (E_R/N_0)\sigma_{R,D}^2$. Then, by substituting (12) in (11), the instantaneous end-to-end SEP can be, with the aid of equations (3), (7), (14) in [15], derived with some manipulations

$$P_e^c \approx \frac{2(M-1)}{M} \left(\mathcal{Q} \left(\sqrt{\frac{6\gamma_{S,R}}{M^2-1}} \right) + \mathcal{Q} \left(\sqrt{\frac{6\gamma_{R,D}}{M^2-1}} \right) \right) - \frac{2(3M-4)}{M} \mathcal{Q} \left(\sqrt{\frac{6\gamma_{S,R}}{M^2-1}} \right) \mathcal{Q} \left(\sqrt{\frac{6\gamma_{R,D}}{M^2-1}} \right). \quad (13)$$

By averaging equation (13) with respect to the PDF of $\gamma_{S,R}$ and $\gamma_{R,D}$, the average end-to-end SEP corresponding to P_e^c can be given by

$$P_e \approx \frac{M-1}{M} \left(2 - \sqrt{\frac{3\bar{\gamma}_{S,R}}{M^2-1+3\bar{\gamma}_{S,R}}} - \sqrt{\frac{3\bar{\gamma}_{R,D}}{M^2-1+3\bar{\gamma}_{R,D}}} \right) - \frac{3M-4}{2M} \left(1 - \sqrt{\frac{3\bar{\gamma}_{S,R}}{M^2-1+3\bar{\gamma}_{S,R}}} \right) \left(1 - \sqrt{\frac{3\bar{\gamma}_{R,D}}{M^2-1+3\bar{\gamma}_{R,D}}} \right). \quad (14)$$

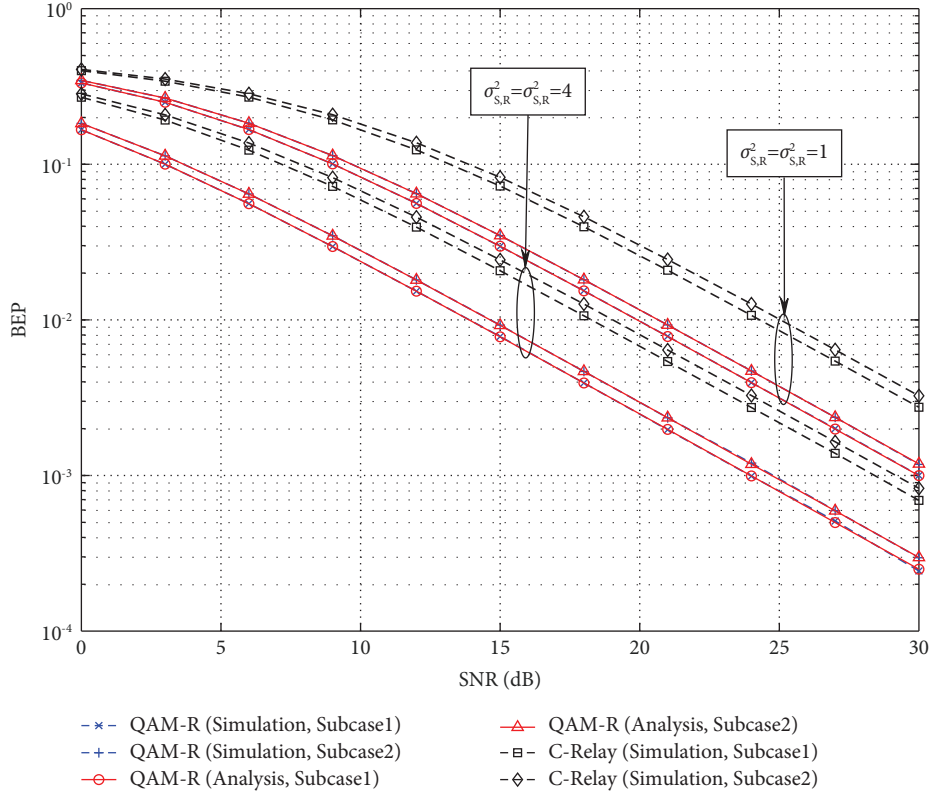


FIGURE 4: Performance comparison between QAM-R and C-Relay under Case 2.

Throughout the paper, we assume that Gray code is used in symbol mapping, so the corresponding end-to-end BEP is

$$P_b \approx \frac{P_e}{\log_2 M}. \quad (15)$$

Especially, since there are only two adjacent decision regions, the approximation in (15) for binary modulation (i.e., $M=2$) becomes the exact expression as follow:

$$P_b = \frac{1}{2} \left(1 - \sqrt{\frac{\bar{\gamma}_{S,R} \bar{\gamma}_{R,D}}{((1 + \bar{\gamma}_{S,R})(1 + \bar{\gamma}_{R,D}))}} \right). \quad (16)$$

4. Numerical Results

We now verify the analytical results and make comparisons with the conventional method. In the simulation, a frame consisting of 128 information symbols is transmitted through a Rayleigh flat fading channel. The channel is also considered as slow fading that remains constant over the whole frame interval. For the sake of fairness, we consider all the schemes have the same bandwidth and power.

We compare our scheme with conventional relay (C-Relay) versus end-to-end BEP under three different cases, namely, Case 1 in which the modulation mode is 4-QAM with distributed mode for QAM-R and binary phase shift keying (BPSK) for C-Relay, Case 2 in which the modulation mode is the same as Case 1 for QAM-R and quadrature phase shift keying (QPSK) for C-Relay and Case 3 in which

the modulation mode is 16-QAM with distributed mode for QAM-R and 16-QAM for C-Relay. For illustrative purposes, let E denote the symbol energy of the whole system, and then we further divide each case into two subcases: subcase 1 which adopts equal power allocation (i.e., $E_S = E_R = 0.5E$) and subcase 2 which adopts unequal power allocation with a power distribution ratio of 3:7 (i.e., $E_S = 0.3E$, $E_R = 0.7E$). Without loss of generality, we assume the variance of AWGN is $N_0 = 1$.

First, we consider Case 1. Since the modulation of QAM-R is MQAM for the whole system but MPAM for SN and RN, respectively, Case 1 is the most basic case. As shown in Figure 3, although QAM-R has a BEP performance penalty of about 3 dB relative to C-Relay, it nearly doubles the transmission rate of the latter for QAM-R works in CCFD mode whereas C-Relay works in HD mode. Second, Figure 4 plots the BEP performance comparison between QAM-R and C-Relay under Case 2 conditions. It can be seen that QAM-R outperforms C-Relay when they both adopting QPSK (i.e., 4-QAM), despite the two schemes have almost the same transmission rate. That is because although the modulation order of C-Relay under Case 2 is twice as that of QAM-R, the latter works in CCFD mode. Moreover, we notice that the numerical results match the exact BEP expression obtained from equation. (16) very well for both Case 1 and Case 2. Third, we provide MQAM to make comparison between QAM-R and C-Relay in Case 3. Figure 5 further confirms the similar results as in Case 2 in terms of BEP performance gain and, especially, shows that QAM-R performs even better in the low range of SNR when adopting higher

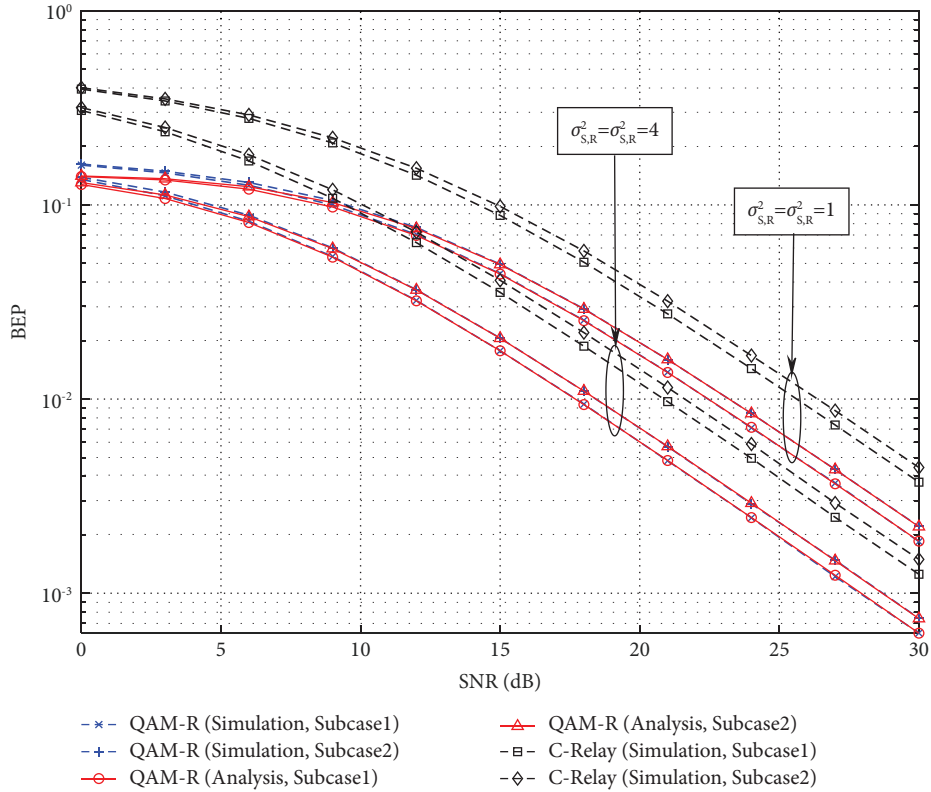


FIGURE 5: Performance comparison between QAM-R and C-Relay under Case 3.

modulation order. It also can be seen from Figure 5 that there is almost no difference in BEP performance between the approximation expression obtained from equation (15) and the simulation results except when SNR is very low, indicating that our approximation formula is quite tight. Taken together, we conclude that our approach has the obvious advantage of tradeoff between spectrum effectiveness and transmission reliability.

To gain more insight, from the respective subcases of all the three case's figures, we find that the equal power allocation is better than the unequal. This reveals that, in practical application, we should try to select the communication node as RN which is nearly equidistant from SN and DN. We can also observe the variances of CFCs have a significant impact on the system, namely, that the performance of $\sigma_{S,R}^2 = \sigma_{R,D}^2 = 4$ is better than that of $\sigma_{S,R}^2 = \sigma_{R,D}^2 = 1$. Besides performance gain, we should notice that realization of QAM-R is just through the different usage mode of modulation constellation, without extraspaces or more complicated hardware/software modules, whereas they are indispensable elements of the traditional SIC.

5. Conclusion

This paper proposes a QAM-R scheme by splitting the entire QAM constellation into two dimensions and then assigning them to source node and relay node, respectively. The proposed approach has the advantage of easy implementation and is immune to the size of transceivers, so it fits in well with the particularities of the small-size devices to

realize CCFD-R mode. It is shown that from both theoretical and numerical results, QAM-R can achieve a good balance between transmission rate and reliability. Looking ahead, numerous small-size devices will undoubtedly appear with the arrival of the IoT era and, hence, QAM-R is valuable and has a broad application prospect.

Data Availability

The data used to support the findings of this study are available from the corresponding author upon reasonable request.

Disclosure

Haiyang Ding is with the Youth Innovation Team of Shaanxi Universities.

Conflicts of Interest

The authors declare that they have no conflicts of interest.

Acknowledgments

This work was supported in part by the Natural Science Basic Research Plan in Shaanxi Province of China (Grant nos. 2020JM-639 and 2022JM-392), and it was also supported in part by the National Key R&D Program of China under Grant 2018YFE0100500, by the National Natural Science Foundation of China under Grants 61871387, and by 2021

Youth Innovation Team Construction Scientific Research Project of Shaanxi Education Department (Grant no. 21JP105).

References

- [1] Z. Zhang, X. Chai, K. Long, A. V. Vasilakos, and L. Hanzo, "Full duplex techniques for 5G networks: self-interference cancellation, protocol design, and relay selection," *IEEE Communications Magazine*, vol. 53, no. 5, pp. 128–137, 2015.
- [2] G. Liu, F. R. Yu, H. Ji, V. C. M. Leung, and X. Li, "In-band full-duplex relaying: a survey, research issues and challenges," *IEEE Communications Surveys & Tutorials*, vol. 17, no. 2, pp. 500–524, 2015.
- [3] E. Everett, A. Sahai, and A. Sabharwal, "Passive self-interference suppression for full-duplex infrastructure nodes," *IEEE Transactions on Wireless Communications*, vol. 13, no. 2, pp. 680–694, 2014.
- [4] B. C. Nguyen, L. The Dung, T. M. Hoang, X. N. Tran, and T. Kim, "Impacts of imperfect CSI and transceiver hardware noise on the performance of full-duplex DF relay system with multi-antenna terminals over Nakagami-m fading channels," *IEEE Transactions on Communications*, vol. 69, no. 10, pp. 7094–7107, 2021.
- [5] A. Hamza, A. Nagulu, A. F. Davidson et al., "A code-domain, in-band, full-duplex wireless communication link with greater than 100-db rejection," *IEEE Transactions on Microwave Theory and Techniques*, vol. 69, no. 1, pp. 955–968, 2021.
- [6] D. C. Nguyen, M. Ding, P. N. Pathirana et al., "6G Internet of Things: a comprehensive survey," *IEEE Internet of Things Journal*, vol. 9, no. 1, pp. 359–383, 2022.
- [7] P. T. Tin, T. N. Nguyen, D. H. Tran, M. Voznak, V. D. Phan, and S. Chatzinotas, "Performance enhancement for full-duplex relaying with time-switching-based SWIPT in wireless sensors networks," *Sensors*, vol. 21, no. 11, p. 3847, 2021.
- [8] X. Liu, Y. Jia, Z. Wen, J. Zou, and S. Li, "Beamforming design for full-duplex SWIPT with co-channel interference in wireless sensor systems," *Sensors*, vol. 18, no. 10, p. 3362, 2018.
- [9] W. Duan, Y. Ji, J. Hou, B. Zhuo, M. Wen, and G. Zhang, "Partial-DF full-duplex D2D-NOMA systems for IoT with/without an eavesdropper," *IEEE Internet of Things Journal*, vol. 8, no. 8, pp. 6154–6166, 2021.
- [10] V. Mahinthan, J. W. Mark, and X. Shen, "A cooperative diversity scheme based on quadrature signaling," *IEEE Transactions on Wireless Communications*, vol. 6, no. 1, pp. 41–45, 2007.
- [11] V. Mahinthan, J. W. Mark, and X. Shen, "Performance analysis and power allocation for M-QAM cooperative diversity systems," *IEEE Transactions on Wireless Communications*, vol. 9, no. 3, pp. 1237–1247, 2010.
- [12] X. Li, L. Deng, Y. Zhang, and S. Chen, "A novel self-interference cancellation technique based on operating-point-optimized optical IQ modulator for co-frequency co-time full duplex wireless communication," in *Proceedings of the 2019 IEEE Optical Fiber Communications Conference and Exhibition (OFC)*, pp. 1–3, San Diego, USA, March 2019.
- [13] A. Goldsmith, *Wireless Communications*, Cambridge University Press, New York, USA, 2005.
- [14] K. Cho and D. Yoon, "On the general BER expression of one- and two-dimensional amplitude modulations," *IEEE Transactions on Communications*, vol. 50, no. 7, pp. 1074–1080, 2002.
- [15] J. G. Proakis, *Digital Communications*, McGraw-Hill Companies, Inc, New York, USA, 4th edition, 2001.